Earth and Planetary Science Letters 298 (2010) 367–376

Contents lists available at ScienceDirect

Earth and Planetary Science Letters

journal homepage: www.elsevier.com/locate/epsl

Constraints on Hadean geodynamics from mineral inclusions in >4 Ga zircons

Michelle D. Hopkins *, T. Mark Harrison, Craig E. Manning

Department of Earth and Space Sciences, University of California, Los Angeles, CA, 90095-1567, USA

ARTICLE INFO

Article history:
Received 6 May 2010
Received in revised form 29 July 2010
Accepted 9 August 2010
Available online 15 September 2010

Editor: R.W. Carlson

Keywords:
zircon
Hadean
inclusion
thermobarometry
U–Pb
Jack Hills

ABSTRACT

The inclusion mineralogy of 1450 zircons over 4 billion years in age from the Jack Hills, Western Australia, was characterized for composition and phase assemblage. Results confirm that the inclusion population of these largely igneous zircons is dominated by muscovite and quartz (~75%). If the inclusions are original to the igneous zircons, this observation alone restricts the host melts to formation at pressure–temperature (*P*–*T*) conditions of ~650–800 °C and >4 kbar. Several lines of evidence support the view that most of the analyzed mineral inclusions are primary, including their lack of association with cracks, magmatic crystal forms, and lack of exchange with fuchsitic (Cr-rich) micas in the host conglomerate. The application of Ti-in-zircon thermometry, and phengite, Ti-in-quartz, and Al-in-hornblende barometry to these inclusion assemblages yields estimates of magmatic *P*–*T* conditions from 5 to >12 kbar and 700 ± 40 °C. These data indicate zircon formation along geotherms of ≤60 °C/km and imply conductive near-surface heat flow of <40 to 85 mW/m^2— a range that is substantially lower than most estimates of global Hadean heat flow. Of the possible environments capable of generating melting under such locally low heat flow early in Earth history, underthrusting, possibly in a manner similar to modern convergent margins, appears most consistent with numerous other geochemical constraints derived from investigation of Hadean zircons.

1. Introduction

Detrital zircons in quartzites from the Jack Hills and Mt. Narryer localities of the Narryer Gneiss Complex (NGC), Western Australia, include the oldest known terrestrial materials (up to 4.38 Ga; Holden et al., 2009) making them the only available record of terrestrial environmental conditions for much of the Hadean eon (ca. >3.85 Ga). After more than a quarter of a century of study (Froude et al., 1983; Compston and Pidgeon, 1986), significant strides have been made to constrain processes during the first 500 Ma of Earth history using these ancient grains (Mojzsis et al., 2001; Peck et al., 2001; Wilde et al., 2001; Cavosie et al., 2004; Turner et al., 2004; Amelin, 2005; Cavosie et al., 2005; Harrison et al., 2005; Watson and Harrison, 2005; Harrison and Schmitt, 2007; Harrison et al., 2007a; Menneken et al., 2007; Trail et al., 2007a,b; Turner et al., 2007; Caro et al., 2008; Harrison et al., 2008; Hopkins et al., 2008; Harrison, 2009).

Geochemical studies of NGC zircons have provided some insights into the type of environments in which these zircons formed and hence of key geological parameters for the Hadean Earth. For example, mineral inclusions within zircons can record the chemical composition of the parental melts and provide information about the initial magmatic conditions under which they formed. From an examination of over 400 inclusion-bearing Hadean zircons from Jack Hills, Hopkins et al. (2008) found that inclusion assemblages are dominated by quartz and muscovite. Their thermobarometric results on 4.02–4.19-Ga inclusion-bearing zircons constrained their magmatic formation conditions to ~700 °C and ~7 kbar, implying a near-surface heat flow of ~80 mWm^{-2}. As this is three to five times lower than estimates of Hadean global heat flow (e.g., Sleep, 2000), they argued that the magmas from which zircons crystallized likely formed in an underthrust environment, perhaps similar to modern convergent margins. In this paper, we revisit this approach with an expanded database of thermobarometric results from Hadean Jack Hills zircon inclusion assemblages as a further test of this hypothesis.

2. Previous inclusion studies of NGC zircons

Minerals and melt trapped during the growth of host phases from magmas can record information about the conditions under which they formed (Schiano, 2003). For example, the mineralogical character of inclusions can yield information about magma chemistry and detailed chemical analyses of these trapped phases can provide quantitative estimates of the pressure and temperature of formation (Thomas et al., 2003). Being able to distinguish whether a mineral trapped in a host phase is indeed a primary inclusion or whether it was produced subsolidus by some non-igneous mechanism is key to such interpretations. Inclusions chosen for analysis must not be associated with imperfections within the host phase; this entails any inclusions near or along cracks or that cross growth zone boundaries

* Corresponding author. Present address: Department of Geological Sciences, University of Colorado, Boulder, CO, 80309-0309, USA. Tel.: +1 303 492 5014; fax: +1 303 492 2606.
E-mail address: michelle.hopkins@colorado.edu (M.D. Hopkins).

0012-821X/$ – see front matter
doi:10.1016/j.epsl.2010.08.010

within the host phase. Furthermore, alterations to the host rocks have the potential to chemically alter mineral inclusions or create new ones, and thus not record primary magmatic conditions.

Previous studies characterizing the inclusion mineralogy of NGC detrital zircons (Maas et al., 1992; Chen et al., 1988; Trail et al., 2004; Cavosie et al., 2004; Menneken et al., 2007; Trail et al., 2007a; Hopkins et al., 2008) documented the presence of quartz, apatite, monazite, K-feldspar, xenotime, rutile, biotite, muscovite, chlorite, FeOOH, Ni-rich pyrite, thorite, amphibole and feldspar. Maas et al. (1992) reported a 40 μm polymineralic "granite" inclusion mainly consisting of quartz with the remainder K-feldspar, biotite, chlorite, and amphibole. The inclusion assemblage quartz, albite, muscovite and biotite was also found (Chen et al., 1998), indicating an origin from hydrous granitoid magmas (Chupin et al. 1998). Monazite and muscovite inclusions were documented by Trail et al. (2004, 2007a) further suggesting a peraluminous magma source. This evidence suggests that the zircon host melts were generally hydrous, meta- and peraluminous granitoid magmas and that perhaps the protolith originated in the presence of water and sedimentary cycling (Mojzsis et al., 2001). Microdiamond inclusions (Menneken et al., 2007) reported in Jack Hills zircons imply a relatively thick, cool continental lithosphere and crust–mantle interactions prior to 4 Ga. It is noted that no other high-pressure minerals such as garnet, coesite, or kyanite have been reported for these ancient zircons which leaves open the possibility that these microdiamonds may not be primary inclusions. Hopkins et al. (2008) identified a sufficiently large suite of inclusions to quantify entrapment conditions by characterizing the pressure and temperature conditions of their formation using thermobarometry.

3. Analytical details

3.1. Sample collection and preparation

Hadean zircons from the Jack Hills were deposited at ca. 3 Ga within a thick (>2 km) series of siliciclastic fan-delta deposits fault-bounded along the northwest margin of the progenitor to the Yilgarn craton (Spaggiari et al., 2007). This study examines zircons found in an outcrop of quartz-rich metasedimentary conglomerate collected from a ~300 m^2 area in the Erawondoo locality where the first ancient zircons were discovered in Jack Hills (Compston and Pidgeon, 1986). Zircons were separated, and then hand-picked and cast in 1 in. diameter epoxy disks in 20×20 rows and columns along with AS-3 zircon standards (Paces and Miller, 1993). Mounts were abraded on 1200 grit carbide paper to expose interior surfaces and then polished using 1 μm diamond paste. One hundred and twenty-nine zircon mounts (RSES55–RSES181) containing ~52,000 zircons, about 1500 of which have Hadean U–Pb ages (Holden et al., 2009), were selected and examined for mineral inclusion characterization within the >4.0 Ga zircons. Thin Au coats applied for the geochronological analyses were stripped from the mounts using an iodine chloride solution, cleaned with methanol and distilled water, and coated with a thin layer of carbon for scanning electron microscope (SEM) imaging and electron probe microanalyzer (EPMA) quantitative elemental analysis.

3.2. Electron imaging and analysis

NGC zircons hosting inclusions were documented with a LEO 1430VP SEM for secondary electron (SE), backscatter electron (BSE), and cathodoluminescence (CL) imaging to determine which grains were large enough to undertake meaningful EPMA chemical analyses. The newly documented inclusion population was more than triple that of Hopkins et al. (2008), providing 1450 pre-4 Ga NGC zircons for examination. Optical examination and limited Raman confocal imaging suggest that virtually all Hadean Jack Hills zircons contain inclusions. Of the examined zircons, 156 contained inclusions that intersected the polished surface and hence did not require further polishing. BSE imaging can provide information about the distribution of different elements and can therefore be used to quickly identify if inclusions are present. Once inclusions are located, they are chemically characterized using energy dispersion X-ray spectroscopy (EDS) to identify the type of each inclusion. CL images were obtained for some zircons to provide information about zircon growth structure. The type and abundance of inclusions determined by EDS were (in brackets: number, average size, and size range): 43% quartz (67, ~14 μm, and 4–30 μm); 36% muscovite (56, ~5 μm, and 1–20 μm); 12% biotite (18, ~5 μm, and 2–10 μm); 3% apatite (5, ~4 μm, and 2–10 μm); 2.5% hornblende (4, ~7.5 μm, and 6–10 μm); 1% rutile (2, ~9 μm, and 8–10 μm); 1% REE oxide (2, ~15 μm, and 14–16 μm); 0.5% monazite (1 and ~10 μm); 0.5% albite (1 and ~4 μm); 0.5% ilmenite (1 and ~25 μm). Notably, even though this current report has tripled the number of NGC zircons examined for mineral inclusions, we have not identified diamonds or other ultrahigh pressure minerals in the many hundreds of Hadean zircons so far examined.

Individual inclusions large enough (i.e., >5–15 μm) to be accurately chemically analyzed were selected for EPMA quantitative elemental analysis. Chemical compositions of each inclusion were obtained *in situ* on either a JEOL 8200 (University of Colorado) or a JEOL 8600 (UCLA) high precision electron microprobe. Out of the 156 surface inclusion-bearing zircons examined, only 21 (17 including muscovite, three quartz, and one hornblende) met the criteria for chemical analysis and were relevant for barometric studies (see images in Supplementary Online Materials, Fig. 1). The 17 muscovite-containing inclusions, in many cases associated with quartz, biotite and other phases, were analyzed by EPMA for a range of major elements and chromium content (e.g., Figs. 2 and 3). Muscovite EPMA data were normalized to 95% total (i.e., 5% H_2O) and converted to structural formula (e.g., Deer et al., 1962) found, in all cases, to be consistent with white mica. Thirteen out of the seventeen muscovites (Group 1) contain S_{pfu} (normalized to 11 oxygens) values with the range 3.09–3.23 while the other four (Group 2) yielded higher S_{pfu} values (3.42–3.46) (Fig. 1, Table 1). All results are consistent with the muscovite structural formula (Deer et al., 1962) and Na loss appears to be minor. Three large quartz inclusions were analyzed for Ti content using an ion microprobe. The sole hornblende inclusion, reported in Hopkins et al. (2008) (Fig. 4), contains an Al content (i.e., sum of $Al^{IV}+Al^{VI}$ per 13 cations) of 2.25.

3.3. Ti-in-zircon thermometry

The Ti-in-zircon thermometer (Watson and Harrison, 2005; Ferry and Watson, 2007) permits zircon crystallization temperature to be

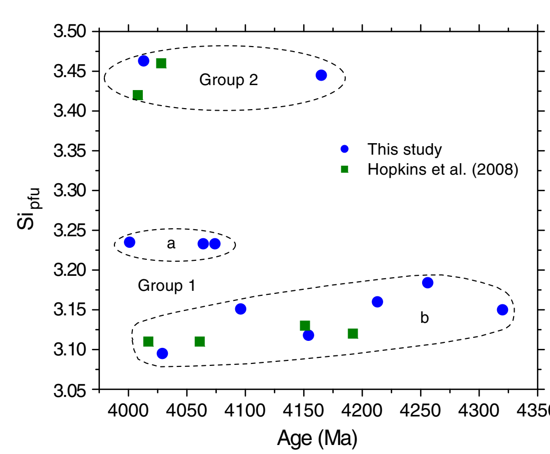

Fig. 1. Plot of Si_{pfu} (calculated from EMPA analyses using the structural formula for muscovite) vs. Pb–Pb age showing the broad clustering of data in high (ca. 3.45) and low (3.1–3.25) Si_{pfu} groupings.

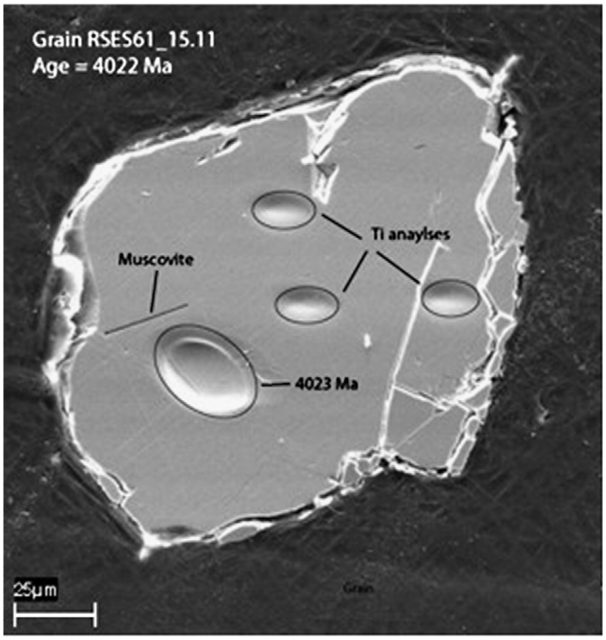

Fig. 2. SEM image of zircon RSES61_15.11 showing high-aspect-ratio muscovite inclusion interpreted to indicate trapping of a magmatic crystal during zircon growth. Positions of U–Pb and Ti analyses also shown.

calculated provided the activities of quartz and rutile can be estimated. For a zircon that coexists with rutile and quartz ($a_{SiO2} \approx a_{TiO2} \approx 1$) an accurate temperature (i.e. ±20 °C) can be obtained. In this study, 16 of the 17 NGC inclusion-bearing zircons were analyzed for Ti concentration using a CAMECA *ims*1270 ion microprobe. Resulting crystallization temperatures range from 648 to 798 °C (Table 1) with an average temperature of 706±38 °C. Ti contamination along crystal imperfections and cracks likely explain the higher temperature datum (i.e., 798 °C) (Harrison and Schmitt, 2007). A limitation in applying this thermometer to detrital NGC zircons is the unknown a_{TiO2} of the parent magma. Although TiO_2 activities in crustal rocks are generally high (e.g., Ghent and Stout, 1984; Kapp et al., 2009), unless co-crystallization with rutile can be established, this temperature is considered a minimum. However, an NGC zircon with an inclusion containing coexisting rutile and quartz (RSES177_5.7) yields a crystallization temperature (667±15 °C) very similar to the population average (680±25 °C; Watson and Harrison, 2005). The implication of this apparent limitation is discussed in Section 4.2.

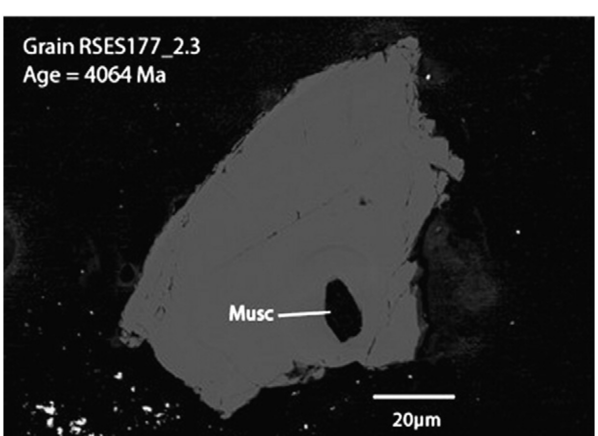

Fig. 3. BSE image of zircon RSES177_2.3 showing near hexagonal muscovite inclusion interpreted to reflect incorporation of a muscovite book during zircon crystallization.

3.4. Phengite barometry

Experimental studies of phengite *P–T* stability in granitic systems (Velde, 1965,1967; Massonne and Schreyer, 1987) show that the miscibility of muscovite towards celadonite (with rising Si^{4+} content) increases linearly with pressure, and thus is a useful geobarometer. Thermodynamic properties of white mica based on high-pressure experiments on Al-celadonite endmembers (Massonne and Szpurka, 1997) constrain isopleths of Si content as a function of *P–T*. These thermodynamic properties were incorporated into THERMOCALC (version 3.26; Holland and Powell, 1998; White et al., 2001), permitting construction of pseudosections for relevant rock compositions. In this study we selected the Bullenbalong cordierite granite (Chappell, 1996) as a representative peraluminous granitoid. We used the same composition modeled by McLaren et al. (2006, their Fig. 8): SiO_2, 75.13; Al_2O_3, 9.62; CaO, 2.69; MgO, 3.67; FeO, 4.27; K_2O, 2.55; Na_2O, 2.07; and H_2O, 6.00 (oxides in mol%). Si_{pfu} isopleths were calculated as a function of *P* and *T* using a Na-free model (Coogon and Holland, 2002), modified to include ideal mixing of Fe and Mg on octahedral sites. Note that incorporation of Na mixing for K yields a pressure ~1 kbar higher for a given Si content (Coogon and Holland, 2002). Group 1 muscovites range in Si_{pfu} from 3.11 to 3.24 with Group 2 muscovite yielding higher values of ~3.4. Using the T_{zir} calculated for each grain, Group 1 formation pressures between 6 and 9 kbar are indicated (Table 1). With one exception, Group 1 muscovites have Si_{pfu} consistent with the predicted stability field of muscovite in the model S-type granite (Fig. 5). As the Group 2 micas are restricted thus far to ages younger than 4.2 Ga, it remains possible that the pressure range of possible crustal types sampled by the Hadean Jack Hills zircons increased with time but the dataset is still too sparse to further speculate on this. Uncertainties in the derived pressures combine errors in the thermodynamic model and electron microprobe data; while the former are difficult to quantify in our approach, variations in key compositional parameters (most importantly, SiO_2) by ±1% translate to no more than ±0.015 Si_{pfu}. Given the spacing and slopes of Si_{pfu} isopleths in Figure 5, this translates to a maximum of about ±0.8 kbar. Varying the bulk composition of modeled peraluminous silicic melts does not affect the results, provided that Na/K is low. This indicates that the muscovite composition predicted by THERMOCALC is controlled not by bulk composition but rather by the solid solution model.

Hopkins et al. (2008) noted that Group 2 micas with Si_{pfu} of ~3.45 are correspondingly rich in Fe. This population persists in our new analyses (Fig. 1; Table 1). Following Hopkins et al. (2008), we do not use these muscovites in our thermodynamic calculations because the imprecisely known valance state and mixing properties of Fe in white mica preclude accurate pressure assignment via the THERMOCALC model. However, Curetti et al. (2008) reported a correlation between pressure (established independent of the Si_{pfu} content) and Si_{pfu} in a large suite of natural white micas which could be used as an alternative to THERMOCALC at high pressures. Their analysis, however, contains no evaluation of compositional parameters other than Si_{pfu} and does not include the covariation of Si_{pfu} with temperature. Although their database contains some cases in which variable Si contents are not due to pressure-dependent Tschermak substitution alone (e.g., Trotet et al., 2001), overall we note that Si_{pfu} interval equivalent to that of Group 2 white micas (i.e., 3.42–3.46) yields pressures of 18±9 kbar (Curetti et al., 2008) and are thus broadly consistent with limited extrapolation of the thermodynamic model. For this reason, we assign Group 2 micas a nominal pressure of >12 kbar. Note that the zircon thermometer requires a correction at high pressures and may require re-calibration at conditions >20 kbar (Ferriss et al., 2008).

Table 1
EMPA analyses of seventeen muscovites inclusions within Hadean zircons. Si_{pfu} (normalized to 11 oxygens) values, crystallization temperatures, formation pressures, and heat flows are also reported for each grain.

Sample	RSES55_6.15	RSES61_10.8	RSES67_3.2	RSES67_15.16	RSES67_19.5	RSES77_5.7	RSES73_6.9	RSES117_11.16
Age (Ma)	4017	4028	4008	4192	4151	4061	4320	4213
SiO_2	47.5	51.2	50.62	45.77	46.67	46.46	46.89	47.39
TiO_2	0.4	0.22	1.52	0.4	0.19	0.4	0.47	0.03
Al_2O_3	35.69	26.3	25.36	34.14	34.55	34.84	33.66	35.17
MgO	0.92	1.68	1.33	0.71	0.93	1.11	0.83	0.12
CaO	0.05	0.08	1.29	0.03	0.05	0	0.02	0.06
MnO	0.01	0.05	0	0	0	0.02	0.02	0
ΣFe as FeO	1.73	6.37	4.12	1.02	1.52	1.3	1.38	1.45
Na_2O	0.45	0.04	1.29	0.5	0.42	0.36	0.29	1.07
K_2O	9.51	8.44	9.69	9.92	9.49	9.8	10.25	8.18
Cr_2O_3	–	0.03	0	0	0	–	–	–
Total	96.26	94.39	95.2	92.5	93.82	94.28	93.81	93.47
Si_{pfu}/11 O	3.11	3.46	3.42	3.12	3.13	3.11	3.15	3.16
T (°C)	695	693	745	723	665	667	725	700
P (kbar)	6.6	>12	>12	7.6	6.5	6	8.7	8
HF (W/m^2)	0.077	<0.042	<0.046	0.07	0.075	0.082	0.061	0.064

Sample	RSES175_6.1	RSES175_8.11	RSES176_19.4	RSES177_2.3	RSES177_10.17	RSES178_7.17	RSES180_5.7	RSES180_6.12	RSES181_20.12
Age (Ma)	4013	4096	4001	4064	4154	4165	4074	4029	4256
SiO_2	52.66	47.38	47.75	49.03	47.04	51.48	48.21	46.4	48.01
TiO_2	0.02	0.81	2.21	0.23	0.45	0.22	0.17	0.13	0.28
Al_2O_3	29.33	33.69	30.66	32.84	35.27	26.3	32.98	34.99	33.94
MgO	1.39	0.59	1.11	2.03	0.67	2.17	1.44	0.95	1.01
CaO	0.24	0.05	0.01	0.02	0	0.01	0	0.01	0.11
MnO	0.01	0.05	0.01	0.02	0.01	0.07	0.01	0.01	0.01
ΣFe as FeO	2.56	3.9	1.83	1.41	1.73	6.07	0.77	2.57	2.11
Na_2O	0.04	0.47	0.29	0.16	0.33	0	0.23	0.31	0.22
K_2O	8.76	8.02	9.17	8.85	9.47	9.68	9.42	9.62	9.42
Cr_2O_3	0.01	0	0.17	0.32	0.32	0.77	0.05	0.16	0.08
Total	95.01	95	93	94.6	95	96	93.2	95	95.1
Si_{pfu}/11 O	3.46	3.15	3.24	3.23	3.12	3.45	3.23	3.1	3.18
T (°C)	684	660	722	672	692	745	682	738	798
P (kbar)	>12	7.2	9.8	9.8	7	>12	9.5	7.6	10
HF (W/m^2)	<0.042	0.067	0.054	0.05	0.073	<0.046	0.053	0.071	0.059

Electron microprobe results from 17 muscovite inclusions in Hadean Jack Hills zircons.

3.5. Al-in-hornblende barometry

The empirically calibrated Al-in-hornblende barometer is based on a broadly linear correlation between total $Al^{IV}+Al^{VI}$ and estimated pressure in the range 2 to 8 kbar (Hammarstrom and Zen, 1986; Hollister et al., 1987). This granitoid barometer appears generally valid provided quartz, biotite, plagioclase, K feldspar and titanite are present, and Fe/(Fe + Mg) < 0.65 in amphibole. The occurrence of quartz, biotite and plagioclase as inclusions, coupled with low sensitivity to titanite and K feldspar buffering (Anderson and Smith, 1995), motivated Hopkins et al. (2008) to apply the barometer. Using the Anderson and Smith (1995) temperature-dependent calibration, Hopkins et al. (2008) obtained a formation pressure of 7 ± 2 kbar for the sole hornblende inclusion (Fig. 4) they reported which contained [Al] = 2.25 cations per 13 for T_{zir} = 700 °C. While this pressure estimate is supportive of the phengite barometry, it should be taken as highly provisional in view of the difficulty in establishing the presence of the full buffering assemblage, as well as evaluating any fO_2 and Fe^{3+} effects.

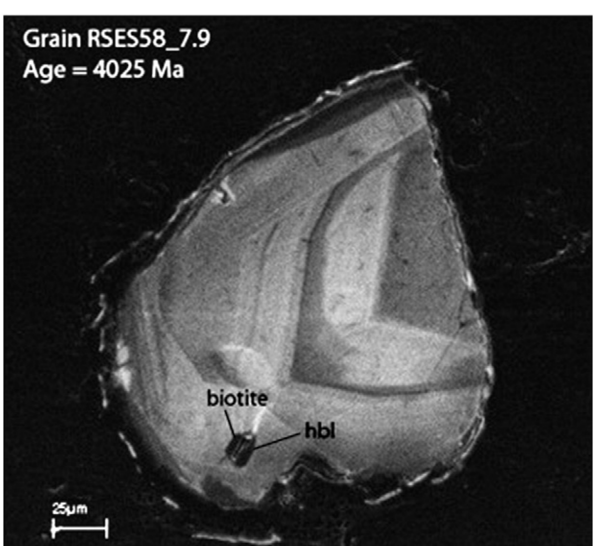

Fig. 4. CL image of zircon RSES58_7.9 showing hornblende + biotite + sphene inclusion.

3.6. Ti-in-quartz barometry

Experimental results of Thomas et al. (2010) revealed strong temperature and pressure dependences on the solubility of Ti in quartz and they thus proposed this system as a thermobarometer. We examined quartz inclusions in Hadean zircons that were sufficiently large (30 to 40 µm) to obtain meaningful analyses and for which Ti in the host zircon had been measured. Unfortunately, the quartz inclusion in the only zircon which contained an analyzed muscovite inclusion, RSES73_6, plucked out in the process of re-polishing.

We standardized for Ti using quartz crystals that had been synthesized in a piston-cylinder apparatus and analyzed for Ti using an electron microprobe by Thomas et al. (2010). They reported Ti concentrations in quartz samples QTiP-7, -14, -38 and -39 of 18 ± 1, 100 ± 2, 380 ± 8 and 813 ± 5 ppm Ti, respectively. We identified

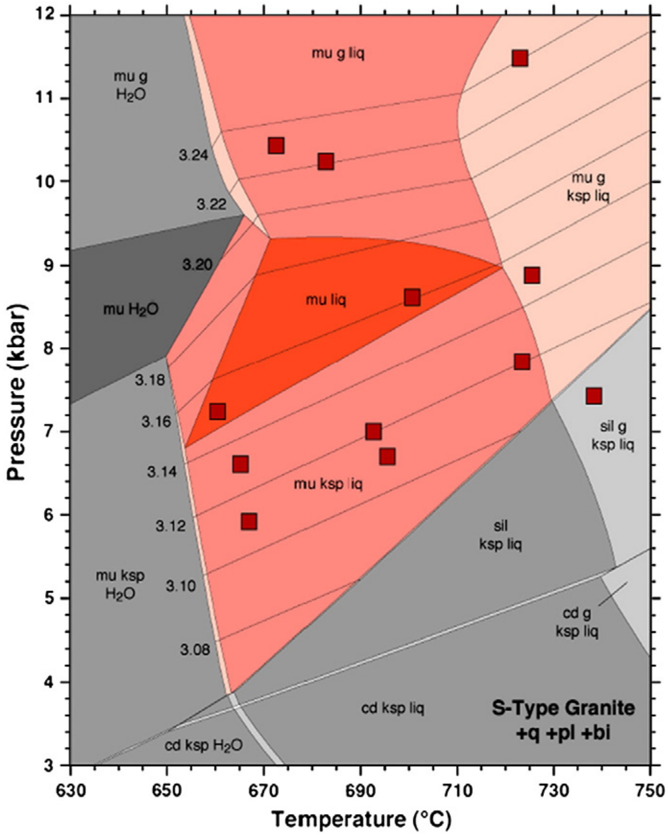

Fig. 5. *P–T* pseudo-section calculated for the Bullenbalong cordierite granite in the presence of q, pl and bio (see text for details). Phase regions depicted with grey shading denote muscovite unstable with melt, whereas red colours show regions where muscovite and melt stably coexist. Darker shading indicates higher variance of phase assemblages. Selected contours of predicted Si content in muscovite (3.08–3.24, in moles per formula unit) are shown with light lines. Squares show *P–T* estimates for analyzed Group 1 micas. Phase abbreviations: bi, biotite; mu, muscovite; sill, sillimanite; q, quartz; pl, plagioclase; liq, granitic melt; g, garnet; cd, cordierite; ksp, K feldspar.

analysis spots on the unknowns by first viewing direct ion images in $^{30}Si^+$ and $^{90}Zr^+$ in order to center the ~30 μm primary ion beam on the quartz inclusion, and then closed the field aperture until $^{90}Zr^+$ counts dropped to background to ensure that secondary Ti^+ ions were only measured from the quartz inclusion. As an illustration of this approach, ion images for zircon RSES181_20 are shown in Figure 4 of the Supplementary Online Materials. $^{48}Ti^+$ and $^{30}Si^+$ were analyzed in peak-hopping mode at a mass resolving power of ~6000, sufficient to separate molecular interference on $^{48}Ti^+$ (Harrison and Schmitt, 2007), using a CAMECA *ims*1270 ion microprobe. The $^{48}Ti^+/^{30}Si^+$ ratios of unknowns were then compared to a linear calibration derived from the standards to determine Ti concentration (Table 2).

Table 2
Ion microprobe analyses of three quartz inclusions within Hadean zircons. Ti (ppm) values, crystallization temperatures, formation pressures, and $^{207}Pb/^{206}Pb$ ages with standard deviation, and inferred heat flows are reported for each grain.

Sample	Ti (qtz) (ppm)	*T* (°C)	*P* (kbar)	$^{207}Pb/^{206}Pb$ age (Ma)	$\pm 1\sigma$ (Ma)	HF (W/m^2)
RSES91_3–18	1.8	633	22	4146	11	0.021
RSES181_20–12	20.6	770	18	4256	5	0.031
RSES57_15–16	8.5	691	19	4082	4	0.027

Ion microprobe results for Ti concentrations from three quartz inclusions in Hadean Jack Hills zircons.

Ti concentrations in quartz from zircons RSES91_3–18, RSES181_20, and RSES57_15–16 ranged from ~2 to 20 ppm, corresponding to pressures of 20 ± 2 kbar using the temperatures calculated from the Ti content of the encompassing zircon.

4. Discussion

4.1. Primary nature of inclusions

Ascertaining whether analyzed mineral inclusions are primary or instead reflect later alteration or even incorporation is challenging but several approaches can be used to evaluate this issue. In assessing the nature of oxygen isotope ratios in Hadean Jack Hills zircons, Cavosie et al. (2005) viewed analyses made "avoiding irregularities such as cracks" as revealing the primary isotopic composition whereas "analyses found to be located on cracks" were rejected. Similarly, none of the analyzed inclusions in this study is associated with visible imperfections in the zircon host such as cracks or growth zone boundaries.

Given that most Hadean Jack Hills zircons show CL evidence of magmatic growth, we would expect primary muscovite to have magmatic crystal forms indicative of primary entrapment from magma rather than irregular structures suggesting ingress along cracks (possibly later healed). Several of the analyzed muscovite inclusions have aspect ratios of 10 to 20, consistent with the distinctive cross-section of muscovite cleavage sheets (Fig. 2). Other muscovites (e.g. Fig. 3) show this mineral's characteristic hexagonal form perpendicular to the c-axis. In the lone hornblende inclusion, the complete assemblage of hornblende + biotite + sphene within a CL zone characteristic of magmatic zoning (Fig. 4) is inconsistent with formation from a pelitic or arenaceous source. In no case was the visible form of any of the analyzed minerals evocative of later alteration (e.g., breakdown products).

The quartzite host of the zircons in our study experienced upper greenschist grade metamorphism at ca. 2.6 Ga (see Spaggiari et al., 2007) and it remains possible that inclusions within the zircons could have formed or been altered at that time. However, one of the primary criteria for field selection of samples is the presence of abundant green layers indicating where chromite has altered to fuchsite (a Cr-mica) on the premise that heavy minerals such as zircon and chromite would likely be co-located in fluvial sediments. Thus Hopkins et al. (2008) argued that a test of this hypothesis would be to examine the relative Cr contents of matrix vs. inclusion dioctahedral micas. They noted that Cr levels in their muscovite inclusions were below detection limits in their EDS analysis method and thus inferred that the included micas had likely remained closed chemical systems. To further evaluate this, we hand-separated fuchsite micas from the host quartzite for quantitative analysis. All fuchsite grains recovered in this fashion were found to be cored by a equant, anhedral chromite grain (Fig. 6). Twelve EMPA analyses of the encompassing fuchsite revealed an average Cr_2O_3 content of 1.4% (Fig. 7; Supplementary Online Materials, Table 1, Fig. 2). In contrast, the thirteen muscovite inclusions analyzed for Cr_2O_3 yielded contents ranging from 0.77 to below the detection limit of 0.04%, with ten <0.2%. These data suggest that the two dioctahedral micas, muscovite and fuchsite, had different origins or grew in distinctly different chemical environments. As the original Cr contents of the mica inclusions are unknown, even the three highest Cr_2O_3 values may be original magmatic values as they include Si_{pfu} values across the range of Group 1a, Group 1b and Group 2 (i.e., RSES177_10.17 $Si_{pfu} = 3.12$; RSES177_2.3 $Si_{pfu} = 3.23$; RSES178_7.17 $Si_{pfu} = 3.45$). Clearly, chemical communication between the host matrix and mica inclusions that passed all other criteria for bona fide inclusion within zircons was, for the most part, quite limited.

The very heterogeneity in Si_{pfu} from ~3.1 to 3.45 argues against widespread, post-depositional metamorphic homogenization. If

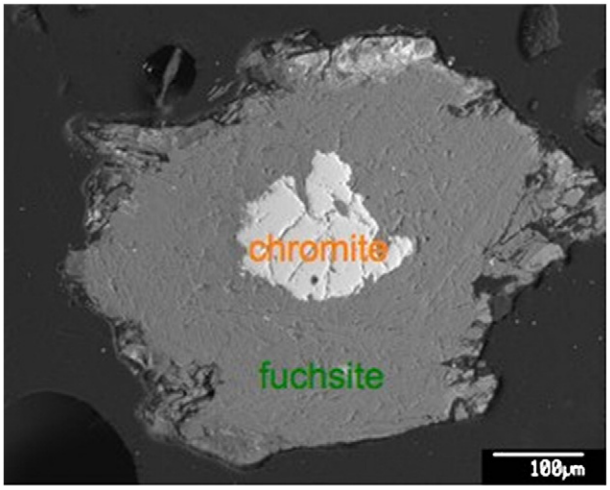

Fig. 6. SEM image showing representative fuchsite grain (see grain 1, Supplementary Online Materials, Fig. 2) cored by detrital chromite from the host quartzite.

muscovite inclusions were largely a consequence of alteration during, say the regional metamorphism at 2.6 Ga, we would expect to see uniform Si/Al ratios in muscovites formed in a 'dirty' quartzite at relatively low (<5 kbar) pressures. The range in Ti content of quartz inclusions is also worth noting in this regard as we know that the host quartzite contains rutile which was highly mobile during the 2.5 Ga metamorphic event (ground mass rutiles yield an average $^{207}Pb/^{206}Pb$ age of 2.3 ± 0.2 Ga; Harrison et al., 2007b). The factor of 10 difference in Ti concentration among the quartz inclusions (Table 2) is further evidence that the inclusion population did not chemically communicate and homogenize with the host rock.

Despite these various lines of evidence supporting a primary magmatic origin for the muscovite, quartz and hornblende inclusions, we have previously noted that isotopic systems in monazite inclusions within zircons from this same quartzite have been reset (Trail et al., 2004; Caro et al., 2008). This likely reflects the very high radioactivity associated with this mineral (see review in Harrison et al., 2002) leading to volume changes that can overcome the confining pressure of the host phase. As such, this behavior has little relevance to the present case. For example, unless all muscovites in this study were fortuitously emplaced into Hadean magmatic zircons during subsolidus reactions that imparted crystal forms characteristics of igneous muscovite together with heterogeneous Si/Al ratios, we can conclude that at least some of these assemblages reflect their formation in a geotherm of ≤60 °C/km as the stability field of muscovite + quartz in peraluminous magmas limits temperatures <800 °C and pressures to >4 kbar (Fig. 5).

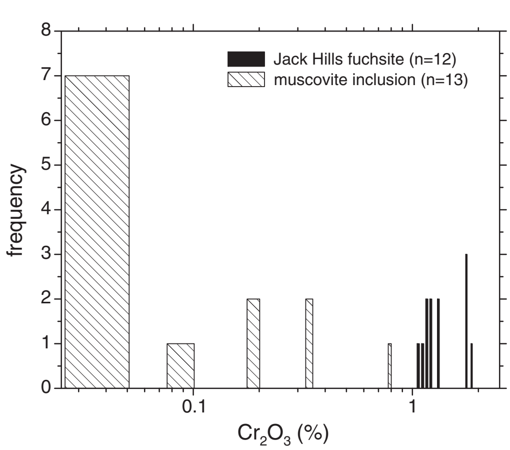

Fig. 7. Measured Cr_2O_3 content of muscovite inclusions in Hadean Jack Hill zircons.

4.2. Geothermal environment of formation

Given that the Hadean Sun was ~30% less luminous than today, surface temperature (T_s) is likely to have been limited to the range 200 to 300 K (e.g., Budyko, 1969; Pierrehumbert, 2005; Zahnle, 2006). We translated individual P–T estimates (Table 1) into apparent thermal gradients (G_m) assuming T_s = 0 °C and an overburden density of 3 g/cm^3. If surface temperatures exceeded 0 °C, then our calculated gradients would be overestimated by ~4 °C/km per 100 °C excess T_s. If the magmas from which the zircons formed had ascended buoyantly from the source of melting prior to crystallization/inclusion trapping, then G_m would also be overestimated (Hopkins et al., 2008). Given the lack of plausible mechanisms that might result in underestimates of G_m, we take the results in Table 1 to represent upper bounds. With regard to accuracy of the zircon thermometer, in all cases save the one previously noted in which rutile is demonstrated to have co-crystallized with zircon, we emphasize that estimates of G_m are broadly parallel to the slope of the Si_{pfu} isopleths in the phengite barometer. Thus underestimating crystallization temperature due to sub-unit a_{TiO2} is largely compensated by lower calculated pressure (i.e., apparent gradients are insensitive to changes in T_{zir}).

Assuming that the host granitoids formed within a thermal boundary layer in which conduction was the dominant heat flow mechanism, we can translate G_m into the average heat flow between the surface and depth of crystallization from Fourier's Law. For a thermal conductivity of 2.5 W/m-°C (Turcotte and Schubert, 2002), our P–T values translate into near-surface (≤60 km) heat flows ranging from <40 to 85 mW/m^2 (Fig. 8; Table 1), with an average of ~60 mW/m^2. This range largely overlaps that of Earth today (Pollack et al., 1993) and is substantially less than that generally inferred for global heat flow during both the Archean (150–200 mW/m^2; Bickle, 1978; Abbott and Hoffman, 1984) and postulated for the Hadean (160–400 mW/m^2; Smith, 1981; Sleep, 2000).

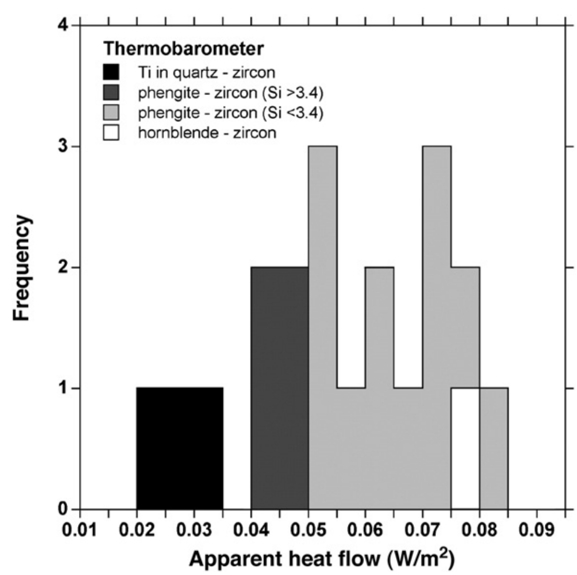

Fig. 8. Summary of apparent near-surface (<30 km) conductive heat flow inferred from thermobarometry of muscovite, quartz and hornblende-bearing inclusions in detrital Hadean zircons. Note Group 2 micas have an apparent heat flow of <0.04 W/m2, therefore these data appear to overlap with Ti-in-qtz data.

4.3. Geochemical constraints

Before evaluating possible physical scenarios consistent with our observations, we first briefly review the constraints on the formation environment of Hadean Jack Hills zircons, derived from their analysis, which any successful model needs to incorporate (see review in Harrison, 2009). To summarize, Hadean Jack Hills zircons:

1) include a population enriched in ^{18}O relative to mantle values suggesting their origin from clay-rich protoliths (Mojzsis et al., 2001; Cavosie et al., 2005; Trail et al., 2007a,b);
2) crystallized at low temperatures (~700 °C) indicating conditions close to or at water saturation (Watson and Harrison, 2005; Harrison et al., 2007a);
3) contain inclusion assemblages that are predominantly magmatic muscovite + quartz + biotite (Hopkins et al., 2008);
4) yield fission Xe isotopes indicating variable fractionation of Pu from U suggesting the presence of aqueous fluids prior to 4 Ga (Turner et al., 2007; Harrison, 2009);
5) yield generally unradiogenic initial $^{176}Hf/^{177}Hf$ ratios, some of which suggest crustal formation as early as ca. 4.5 Ga (Harrison et al., 2005; Blichert-Toft and Albarède, 2008; Harrison et al., 2008);
6) contain geochemical signatures diagnostic of felsic continental rocks (Grimes et al., 2007; Trail et al., 2007a,b; Grimes et al., 2010);
7) contain inclusion assemblages most similar to those in S- and I-type granitoid magmas (Maas et al., 1992; Mojzsis et al., 2001; Hopkins et al., 2008);
8) do not contain UHP phases (Maas et al., 1992; Hopkins et al., 2008; cf. Menneken et al., 2007); and,
9) yield thermobarometric results suggestive of their formation in low (~40–80 mW/m^2) heat flow environments (Hopkins et al., 2008; this study).

4.4. Melting environments

Before focusing on environments most consistent with our observations, we first rule out several that have been proposed as sources for these ancient zircons. Zircons formed from impact melts, assumed to be commonplace during the Hadean, are different from the Hadean population in their high (ca. 800 °C) crystallization temperatures (Darling et al., 2009) and are unlikely to form under near water-saturated conditions (Watson and Harrison, 2005).

Several authors (Galer and Goldstein, 1991; Coogan and Hinton, 2006; Shirey et al., 2008) have proposed a mantle origin (e.g., MORB plagiogranites, mafic igneous complexes, and kimberlites) for Hadean Jack Hills zircons. Such environments, however, yield distinctively different trace element signatures, zircon crystallization temperature and oxygen isotopes spectra relative to the Hadean population (Grimes et al., 2007; Harrison, 2009; Grimes et al., 2010) and produce peraluminous melts and heavy oxygen isotope signatures only in rare circumstances (e.g., Gregory and Taylor, 1981; Rollinson, 2008). Primary zircons produced from tonalite–trondhjemite–granodiorite magmas have broader crystallization temperature spectra than the Hadean population and are not typified by S-type inclusion assemblages (Harrison et al., 2007a; cf. Nutman and Hiess, 2008).

Having ruled out mantle and extraterrestrial origins, we now focus on formation environments most consistent with constraint (9); i.e., formation in low heat flow environments. There are numerous ways for a planet to locally experience near-surface, transient, low heat flow. For example, a thick, stable lithosphere containing low abundances of radioactive elements can result in heat flow as little as one-fourth of the global average (e.g., Superior Province; Mareschal and Jaupart, 2004). However, as this environment is unlikely to be characterized by magmatism, it is unimportant to our discussion.

More appealingly, the core of a near-surface rock mass that rapidly down wells into the mantle is insulated from reaching melting temperatures until attaining relatively high pressure. Thus incipient melting there could arise in an overall low apparent geotherm via 'sagduction' rather than underthrusting (e.g., Gorman et al., 1978). However, to illustrate the limitations of this model in reconciling with evidence obtained from Hadean zircons (i.e., Section 4.3), consider the case of a subsiding block of mafic eclogite. Below ~30 km depth, rock porosities are typically <0.1% (Ingebritsen and Manning, 2002) and thus little free water is available to flux melting. Structural water stored in hydrous minerals is limited to ≤2% of virtually all rocks and is lost progressively via discontinuous, subsolidus dehydration reactions through the greenschist and amphibolite facies (Spear, 1993). This liberated water is likely to ascend from the down-welling into colder, shallower level, rocks. Thus melting is likely to be forestalled until temperatures greatly exceeding that of minimum melting are reached. In the case of complete devolatilization, temperatures of >900 °C would be required for melting of dry rock. Magma produced in this fashion will be characterized by low water and high Zr concentrations and thus lead to formation of zircons characterized by high (>800 °C) crystallization temperatures (Watson and Harrison, 1983). At the least, that temperature spectrum could be expected to show peaks corresponding to the relevant dehydration melting equilibria (e.g., biotite melting at ca. 800 °C, amphibole melting at ca. 900 °C; Spear, 1993). Furthermore, these melts are unlikely to be characterized by the assemblage quartz + muscovite. A sinking slab of pelitic sediment is more appealing in this latter regard but, again, will be limited in the amount of water available to flux melting. For example, sediment containing a 50:50 mixture of muscovite and quartz contains only ~2 wt.% water and dehydration melting of such a protolith produces water-undersaturated melts (e.g., Patiño Douce and Harris, 1998).

What the above models lack is a mechanism to introduce water-rich fluids into fertile source rocks capable of yielding both peraluminous and metaluminous magmas at temperatures close to minimum melting (as required by Ti thermometry) and then sustain the supply of water until the rock's melt fertility is essentially exhausted (thus resulting in the single Hadean zircon peak at ca. 680 °C). The simplest mechanism that appears consistent with all of the relevant constraints (1–9) is melting of mature continental sediment during continuous, submarine underthrusting beneath a stable upper plate capable of long-term (i.e., >4 Ga) preservation of a geologic record. The melting could occur in two scenarios: A, fluxed melting of underthrust sedimentary material, or B, fluxed melting of sediment in the upper plate due to water delivery to the melting site from either the lower plate or degassing of a proximal crystallizing hydrous magma derived from the underthrust environment. In both scenarios, the presence of abundant water, derived from either open porosity at relatively shallow depths or lower plate dehydration, is consistent with constraints 1–4; the mix of source rocks is consistent with constraints 3, 6 and 7; the stable upper plate is required by constraints 3, 5 and 7; melting is consistent with constraints 2, 3, 7, and 8; and an underthrusting regime explains constraint 9.

The choice between the two scenarios depends on the weighting placed on our thermobarometric results. *P*–*T* estimates derived solely from muscovite and zircon compositions constrain crystallization conditions of host magma(s), and yield conditions corresponding to average modern middle crust. If however the pressures derived from Ti-in-quartz barometry and Group II muscovites are also considered, then we speculate that these results could conceivably reflect conditions of melting deep in an upper plate or in an underthrusted plate. Significantly, the *P*–*T* conditions implied by Ti in zircon and in quartz would be consistent with slab-top pressures of modern hot subduction zones at temperatures of wet sediment melting (e.g.

Hermann and Spandler, 2008; Syracuse et al., in press). If correct, this would imply that zircon was on the liquidus from melt generation to crystallization, and that inclusions were trapped both at an early stage, during melting, and later, during crystallization.

4.5. Possible tectonic environment

The model described above is strikingly similar to melt production in a modern convergent margin setting — the only terrestrial magmatic environment characterized by heat flow of around one third of the global average (i.e., the geotherm to the site of andesite production is today typically only ~12 °C/km). It does, however, run contrary to the traditional view that high mantle temperatures extant in early Earth would result in thick (>40 km), fast-spreading oceanic crust that resists subduction (McKenzie and Bickle, 1988; Davies, 1992), potentially leading to trench lock (Sleep, 2000). Thus Hadean plate-tectonic-like behavior has historically been viewed as unlikely.

This interpretation, however, presupposes that the convective vigor of the mantle is a simple function of its temperature and that heat loss is broadly equivalent to its generation. Korenaga (2003, 2006) proposed a radically different scaling between global heat loss and interior temperature in which mantle heat loss relative to that by conduction alone (the Nusselt number, *Nu*) early in Earth history scaled to the Raleigh number (*Ra*; the ratio of buoyancy to dissipative forces) via a negative exponent (i.e., $Nu \propto Ra^{-\gamma}$, where $\gamma = 0.15$). In this regime, high degrees of partial melting resulting from high interior temperature are hypothesized to have profoundly altered the viscosity structure of the upper mantle as the primitive silicate Earth dewatered. The resulting sluggish convection reduces heat loss such that a mantle potential temperature (T_p) of 1600 °C corresponds to a globally averaged heat loss similar to present. Herzberg et al. (2010) provided some support for this model by showing that estimates of mantle potential temperatures from Precambrian non-arc basalts broadly conformed to model predictions (i.e., apparent Archean–Hadean mantle warming suggests that internal heating exceeded surface heat loss).

Relating parameterized calculations of heat loss thorough an oceanic radiator to the regional scale thermal structure of a subduction zone, possibly adjacent a continental backstop, is not straightforward but some constraints are available. For the case previously noted (i.e., $\gamma = 0.15$, $T_p = 1600$ °C) corresponding to ~4 Ga, Korenaga (2006) calculated that a ~140 km thick oceanic lithosphere would become neutrally buoyant in ~120 Ma, implying an average plate velocity of ~2 cm/yr. We have accordingly modeled the thermal structure of an underthrust zone (Grove et al., 2003) in which such a lithospheric slab, after traveling 3000 km from the spreading ridge, is thrust beneath a rigid upper plate containing continental lithosphere extending to 50 km depth. Additional assumptions include: 25° dip, basal and surface continental lithosphere heat fluxes of 30 and 200 mW/m^2, respectively, and a Moho depth of 15 km. Because heat flow in the upper plate in this model is entirely diffusive (i.e., no counter flow), results provide a conservative estimate of the position above the slab at which minimum melting temperatures could arise at depths of 20–30 km. Thus the effective mechanical coupling depth in our simulations (e.g., Tichelaar and Ruff, 1993) occurs at far greater depths (>100 km) than likely for the conditions extant in a Hadean convergent margin. Notwithstanding, we were still able to simulate temperatures of 650 to 750 °C in the hanging wall at depths between 20 and 30 km (i.e., 6 to 9 kbar) corresponding to quasi-steady state apparent geotherms of 20 to 30 °C/km (Supplementary Online Materials, Fig. 3). This well simulates our Group 1 results which indicate zircon crystallization at ca. 700 °C occurred at depths between 6 and 10 kbar.

While not uniquely supportive of the Korenaga (2006) model, our data are consistent with many of its predictions. The one aspect of our model different from modern convergent margins is the requirement for near water-saturated melting. This could reflect a much higher thermal gradient (i.e., 30–40 °C/km vs. ~12 °C/km today) telescoping metamorphic dehydration reactions into a spatially restricted zone (i.e., <10 km vs. 40–50 km) at much shallower depths, enhancing the role of hydrofracturing in transporting abundant, water-rich fluids to the site of melting.

5. Conclusions

Mineralogical and chemical investigations of mineral inclusions in detrital Hadean zircons provide insights into their formation environments provided the inclusions are primary. In this study of zircons from Jack Hills, Western Australia, mineral inclusions used for thermobarometry were found to be unassociated with cracks, show magmatic crystal forms indicative of primary entrapment, and not to have significantly chemically exchanged in their post-depositional environment. An examination of 1450 pre-4.0 Ga, largely igneous, zircons reaffirms that their inclusion population is dominated (~75%) by muscovite and quartz, thus restricting the host melts to pressure–temperature (*P*–*T*) conditions of ~650–800 °C and >4 kbar. Thermobarometric results from seventeen muscovite, three quartz and one hornblende inclusion(s) yield estimates of magmatic *P*–*T* conditions between 5 and >12 kbar and ca. 700 °C. These data imply geotherms to the site of zircon crystallization between ca. 20 and 40 °C/km, corresponding to conductive heat flows ranging between <40 and 85 mW/m^2. This range results in global heat loss estimates that are less than that generated by radioactivity alone. We thus infer that these inclusion-bearing Hadean zircons formed in an environment of suppressed heat flow. Possible formation environments capable of generating melting under suppressed heat flow conditions must also be consistent with numerous constraints derived from other geochemical investigations of Hadean zircons. Our interpretation is that the simplest model that successfully incorporates all relevant constraints is hydrous melting in the hanging wall of thrust faults, possibly in a manner similar to modern convergent margins.

Supplementary materials related to this article can be found online at doi:10.1016/j.epsl.2010.08.010.

Acknowledgements

We acknowledge facility support for the Instrumentation and Facilities Program of the National Science Foundation. We thanks A. Schmitt for assistance with the ion microprobe analyses, F. Kyte and J. Drexler for assistance with the EMPA analyses, and S. Mojzsis for reviewing the manuscript.

References

Abbott, D.H., Hoffman, S.E., 1984. Archean plate tectonics revisited. Part 1. Heat flow, spreading rate, and the age of subducting oceanic lithosphere and their effects on the origin and evolution of continents. Tectonics 3, 429–448.

Amelin, Y., 2005. Sm–Nd systematics of zircon. Chem. Geol. 211, 375–387.

Anderson, J.L., Smith, D.R., 1995. The effect of temperature and fO_2 on the Al-in-hornblende barometer. Am. Mineralog. 80, 549–559.

Bickle, M.J., 1978. Heat loss from the Earth: constraints on Archean tectonics from the relation between geothermal gradients and the rate of plate production. Earth Planet. Sci. Lett. 40, 301–315.

Blichert-Toft, J., Albarède, F., 2008. Hafnium isotopes in Jack Hills zircons and the formation of the Hadean crust. Earth Planet Sci. Lett. 265, 686–702.

Budyko, M.I., 1969. The effect of solar radiation variations on the climate of Earth. Tellus 21, 611–619.

Caro, G., Bennett, V.C., Bourdon, B., Harrison, T.M., Mojzsis, S.J., Harris, J.W., 2008. Precise analysis of $^{142}Nd/^{144}Nd$ in small samples: application to Hadean zircons from Jack Hills (W. Australia) and diamond inclusions from Finsch (S. Africa). Chem. Geol. 247, 253–265.

Cavosie, A.J., Wilde, S.A., Liu, D., Weiblen, P., Valley, J.W., 2004. Internal zoning and U–Th–Pb chemistry of Jack Hills detrital zircons: a mineral record of early Archean to Mesoproterozoic (4348–1576 Ma) magmatism. Precambrian Res 134, 251–279.

Cavosie, A.J., Valley, J.W., Wilde, S.A., 2005. Magmatic $\delta^{18}O$ in 4400–3900 Ma detrital zircons: a record of the alteration and recycling of crust in the Early Archean. Earth Planet. Sci. Lett. 235, 663–681.

Chappell, B.W., 1996. Compositional variation within granite suites of the Lachlan Fold Belt; its causes and implications for the physical state of granite magma. Geol. Soc. Am. Spec. Pap. 315, 159–170.

Chen, Y.D., Price, R.C., White, J.R., 1988. Inclusions in three S-type granites from southeastern Australia. J. Petrol. 30, 1181–1218.

Chupin, S.V., Chupin, V.P., Barton, J.M., Barton, E.S., 1998. Archean melt inclusions in zircon from quartzite and granitic orthogneiss from South Africa: magma compositions and probable sources of protoliths. Eur. J. Mineral. 10, 1241–1251.

Compston, W., Pidgeon, R.T., 1986. Jack Hills, evidence of more very old detrital zircons in Western Australia. Nature 321, 766–769.

Coogan, L.A., Hinton, R.W., 2006. Do the trace element compositions of detrital zircons require Hadean continental crust? Geology 34, 633–636.

Coogon, R., Holland, T.J.B., 2002. Mixing properties of phengitic micas and revised garnet–phengite thermobarometers. J. Metamorph. Geol. 20, 683–696.

Curetti, N., Ferraris, G., Ivaldi, G., 2008. Correlation between crystallization pressure and structural parameters of phengites. Am. Mineral. 93, 451–455.

Darling, J., Storey, C., Hawkesworth, C., 2009. Impact melt sheet zircons and their implications for the Hadean crust. Geology 37, 927–930.

Davies, G.F., 1992. On the emergence of plate-tectonics. Geology 20, 963–966.

Deer, W.A., Howie, R.A., Zussmann, J., 1962. Rock Forming Minerals, II. Sheet Silicates. Longmans, London.

Ferriss, E.D.A., Essene, E.J., Becker, U., 2008. Computational study of the effect of pressure on the Ti-in-zircon geothermometer. Eur. J. Mineral. 20, 745–755.

Ferry, J.M., Watson, E.B., 2007. New thermodynamic models and revised calibrations for the Ti-in-zircon and Zr-in-rutile thermometers. Contrib. Mineral. Petrol. 154, 429–437.

Froude, D.O., Ireland, T.R., Kinny, P.D., Williams, I.S., Compston, W., 1983. Ion microprobe identification of 4, 100–4, 200 Myr-old terrestrial zircons. Nature 304, 616–618.

Galer, S.J.G., Goldstein, S.L., 1991. Early mantle differentiation and its thermal consequences. Geochim. Cosmochim. Acta 55, 227–239.

Ghent, E.D., Stout, M.Z., 1984. TiO_2 activity in metamorphosed pelitic and basic rocks: principles and applications to metamorphism in southeastern Canadian Cordillera. Contrib. Mineral. Petrol. 86, 248–255.

Gorman, B.E., Pearce, T.H., Birkett, T.C., 1978. On the structure of Archaean greenstone belts. Precambrian Res. 6, 23–41.

Gregory, R.T., Taylor, H.P., 1981. An oxygen isotope profile in a section of Cretaceous oceanic-crust, Samail ophiolite, Oman — evidence for $\delta^{18}O$ buffering of the oceans by deep (less-than 5 km) seawater-hydrothermal circulation at Mid-ocean Ridges. J. Geophys. Res. 86, 2737–2755.

Grimes, C.B., John, B.E., Kelemen, P.B., Mazdab, F.K., Wooden, J.L., et al., 2007. Trace element chemistry of zircons from oceanic crust: a method for distinguishing detrital zircon provenance. Geology 35, 643–646.

Grimes, C.B., Ushikubo, T., John, B.E., Valley, J.W., 2010. Uniformly mantle-like d18O in zircons from oceanic plagiogranites and gabbros. Contrib. Mineral. Petrol. doi:10.1007/s00410-010-0519-x.

Grove, M., Lovera, O.M., Harrison, T.M., 2003. Late Cretaceous cooling of the east-central Peninsular Ranges Batholith (33°N): relationships to La Posta pluton emplacement, Laramide shallow subduction, and forearc sedimentation. Geol. Soc. Am. Spec. Pap. 374, 355–380.

Hammarstrom, J.M., Zen, E., 1986. Aluminum in hornblende: an empirical igneous geobarometer. Am. Mineral. 71, 1297–1313.

Harrison, T.M., 2009. The Hadean crust: evidence from >4 Ga zircons. Annu. Rev. Earth Planet. Sci. Lett. 37, 479–505.

Harrison, T.M., Schmitt, A.K., 2007. High sensitivity mapping of Ti distributions in Hadean zircons. Earth Planet. Sci. Lett. 261, 9–19.

Harrison, T.M., Catlos, E.J., Montel, J.M., 2002. U–Th–Pb dating of phosphate minerals. Rev. Mineral. Geochem. 48, 523–558.

Harrison, T.M., Blichert-Toft, J., Müller, W., Albarède, F., Holden, P., Mojzsis, S.J., 2005. Heterogeneous Hadean hafnium: evidence of continental crust at 4.4 to 4.5 Ga. Science 310, 1947–1950.

Harrison, T.M., Watson, E.B., Aikman, A.K., 2007a. Temperature spectra of zircon crystallization in plutonic rocks. Geology 35, 635–638.

Harrison, T.M., Trail, D., Schmitt, A.K., Watson, E.B., 2007b. Rutile ^{207}Pb–^{206}Pb ages in the Jack Hills Quartzite, Western Australia. Goldschmidt Conference Abstracts 2007, p. A383.

Harrison, T.M., Schmitt, A.K., McCulloch, M.T., Lovera, O.M., 2008. Early (≥4.5 Ga) formation of terrestrial crust: Lu-Hf, δ18O, and Ti thermometry results for Hadean zircons. Earth Planet. Sci. Lett. 268, 476–486.

Hermann, J., Spandler, C.J., 2008. Sediment melts at sub-arc depths: an experimental study. J. Petrol. 49, 717–740.

Herzberg, C., Condie, K., Korenaga, J., 2010. Thermal history of the Earth and its petrological expression. Earth Planet. Sci. Lett. 292, 79–88.

Holden, P., Lanc, P., Ireland, T.R., Harrison, T.M., Foster, J.J., Bruce, Z., 2009. Mass-spectrometric mining of Hadean zircons by automated SHRIMP multi-collector and single-collector U/Pb zircon age dating: the first 100, 000 grains. Int. J. Mass Spectrom. Ion Proc. 286, 53–63.

Holland, T.J.B., Powell, R., 1998. An internally consistent thermodynamic data set for phases of petrologic interest. J. Metamorph. Geol. 16, 309–343.

Hollister, L.S., Grissom, G.C., Peters, E.K., Stowell, H.H., Sisson, V.B., 1987. Confirmation of the empirical correlation of Al in hornblende with pressure of solidification of calc-alkaline plutons. Am. Mineral. 72, 231–239.

Hopkins, M., Harrison, T.M., Manning, C.E., 2008. Low heat flow inferred from >4 Gyr zircons suggests Hadean plate boundary interactions. Nature 456, 493–496.

Ingebritsen, S.E., Manning, C.E., 2002. Diffuse fluid flux through orogenic belts: implications for the world ocean. Proc. Natl. Acad. Sci. 99, 9113–9116.

Kapp, P., Manning, C.E., Tropper, P., 2009. Phase-equilibrium constraints on titanite and rutile activities in mafic epidote amphibolites and geobarometry using titanite–rutile equilibria. J. Metamorph. Geol. 27, 509–521.

Korenaga, J., 2003. Energetics of mantle convection and the fate of fossil heat. Geophys. Res. Lett. 30, 1437.

Korenaga, J., 2006. Archean geodynamics and the thermal evolution of Earth. In: Benn, K., Mareschal, J.C., Condie, K. (Eds.), Archean Geodynamics and Environments: AGU Geophysical Monograph Series, 164, pp. 7–32.

Maas, R., Kinny, P.D., Williams, I.S., Froude, D.O., Compston, W., 1992. The Earth's oldest known crust: a geochronological and geochemical study of 3900–4200 Ma old detrital zircons from Mt. Narryer and Jack Hills, Western Australia. Geochim. Cosmochim. Acta 56, 1281–1300.

Mareschal, J.C., Jaupart, C., 2004. Variations of surface heat flow and lithospheric thermal structure beneath the North American craton. Earth Planet. Sci. Lett. 223, 65–77.

Massonne, H.J., Schreyer, W., 1987. Phengite geobarometry based on the limiting assemblage with K-feldspar, phlogopite, and quartz. Contrib. Mineral. Petrol. 96, 212–224.

Massonne, H.J., Szpurka, Z., 1997. Thermodynamic properties of white micas on the basis of high-pressure experiments in the systems K_2O–MgO–Al_2O_3–SiO_2–H_2O and K_2O–FeO–Al_2O_3–SiO_2–H_2O. Lithos 41, 229–250.

McKenzie, D., Bickle, M.J., 1988. The volume and composition of melt generated by extension of the lithosphere. J. Petrol. 29, 625–679.

McLaren, S., Sandiford, M., Powell, R., Neumann, N., Woodhead, J., 2006. Palaeozoic intraplate crustal anatexis in the Mount Painter Province, South Australia: timing, thermal budgets and the role of crustal heat production. J. Petrol. 47, 2281–2302.

Menneken, M., Nemchin, A.A., Geisler, T., Pidgeon, R.T., Wilde, S.A., 2007. Hadean diamonds in zircon from Jack Hills, Western Australia. Nature 448, 917–920.

Mojzsis, S.J., Harrison, T.M., Pidgeon, R.T., 2001. Oxygen-isotope evidence from ancient zircons for liquid water at the Earth's surface 4300 Myr ago. Nature 409, 178–181.

Nutman, A.P., Hiess, J., 2008. A granitic inclusion suite within igneous zircons from a 3.81 Ga tonalite (W. Greenland): restrictions for Hadean crustal evolution studies using detrital zircons. Chem. Geol. 261, 76–81.

Paces, J.B., Miller, J.D., 1993. Precise U–Pb age of Duluth Complex and related mafic intrusions, northeastern Minnesota: geochronological insights into physical, petrogenetic, paleomagnetic, and tectonomagmatic processes associated with the 1.1 Ga midcontinent rift system. J. Geophys. Res. 98, 13, 997–14,013.

Patiño Douce, A., Harris, N., 1998. Experimental constraints on Himalayan anatexis. J. Petrol. 39, 689–710.

Peck, W.H., Valley, J.W., Wilde, S.A., Graham, C.M., 2001. Oxygen isotope ratios and rare earth elements in 3.3 to 4.4 Ga zircons: ion microprobe evidence for high $\delta^{18}O$ continental crust and oceans in the Early Archean. Geochim. Cosmochim. Acta 65, 4215–4229.

Pierrehumbert, R.T., 2005. Climate dynamics of a hard snowball Earth. J. Geophys. Res. 110 doi:10.1029/2004JD005162.

Pollack, H.N., Hurter, S.J., Johnson, J.R., 1993. Heat flow from the earth's interior: analysis of the global data set. Rev. Geophys. 31, 267–280.

Rollinson, H., 2008. Ophiolitic trondhjemites: a possible analogue for Hadean felsic 'crust'. Terra Nova 20, 364–369.

Schiano, P., 2003. Primitive mantle magmas recorded as silicate melt inclusions in igneous minerals. Earth Sci. Rev. 63, 121–144.

Shirey, S.B., Kamber, B.S., Whitehouse, M.J., Mueller, P.A., Basu, A.R., 2008. A review of the isotopic and trace element evidence for mantle and crustal processes in the Hadean and Archean: implications for the onset of plate tectonic subduction. Geol. Soc. Am. Spec. Pap. 440, 1–29.

Sleep, N.L., 2000. Evolution of the mode of convection within terrestrial planets. J. Geophys. Res. 105, 17563–17578.

Smith, J.V., 1981. The first 800 million years of Earth's history. Philos. Trans. R. Soc. London Ser. A 301, 401–422.

Spaggiari, C.V., Pidgeon, R.T., Wilde, S.A., 2007. The Jack Hills greenstone belt, Western Australia: part 2: lithological relationships and implications for the deposition of ≥4.0 Ga detrital zircons. Precambrian Res. 155, 261–286.

Spear, F.S., 1993. Metamorphic Phase Equilibria and Pressure–Temperature–Time–Paths. Mineral. Soc. Amer., Washington D.C.

Syracuse, E.M., van Keken, P.E., Abers, G.A., in press. The global range of subduction zone thermal models. Phys. Earth. Planet. Inter. doi:10.1016/j.pepi.2010.02.004.

Thomas, J.B., Bodnar, R.J., Shimizu, N., Chesner, C.A., 2003. Melt inclusions in zircon. Rev. Mineral. 53, 63–87.

Thomas, J.B., Watson, E.B., Spear, F.S., Shemella, P.T., Nayak, S.K., Lanzirotti, A., 2010. TitaniQ under pressure: the effect of pressure and temperature on the solubility of Ti in quartz. Contrib. Mineral. Petrol. doi:10.1007/s00410-010-0505-3.

Tichelaar, B.W., Ruff, L.J., 1993. Depth of seismic coupling along subduction zones. J. Geophys. Res. 98, 2017–2037.

Trail, D., Mojzsis, S.J., Harrison, T.M., 2004. Inclusion mineralogy of pre-4.0 Ga zircons from Jack Hills, Western Australia: a progress report. Geochim. Cosmochim. Acta 68, A743.

Trail, D., Mojzsis, S.J., Harrison, T.M., 2007a. Thermal events documented in Hadean zircons by ion microprobe depth profiles. Geochim. Cosmochim. Acta 71, 4044–4065.

Trail, D., Mojzsis, S.J., Harrison, T.M., Schmitt, A.K., Watson, E.B., Young, E.D., 2007b. Constraints on Hadean zircon protoliths from oxygen isotopes, REEs and Ti-thermometry. Geochem. Geophys. Geosyst. 8, Q06014 doi:10.1029/2006GC001449.

Trotet, A., Vidal, O., Jolivet, L., 2001. Exhumation of Syros and Sifnos metamorphic rocks (Cyclades, Greece). New constraints on the P–T paths. Eur. J. Mineral. 13, 901–920.
Turcotte, D.L., Schubert, G., 2002. Geodynamics: Applications of Continuum Physics to Geological Problems, 2nd edition. John Wiley, New York.
Turner, G., Harrison, T.M., Holland, G., Mojzsis, S.J., Gilmour, J., 2004. Extinct ^{244}Pu in ancient zircons. Science 306, 89–91.
Turner, G., Busfield, A., Crowther, S., Mojzsis, S.J., Harrison, T.M., Gilmour, J., 2007. Pu–Xe, U–Xe, U–Pb chronology and isotope systematics of ancient zircons fromWestern Australia. Earth Planet. Sci. Lett. 261, 491–499.
Velde, B., 1965. Phengite micas: synthesis, stability, and natural occurrence. Am. J. Sci. 263, 886–913.
Velde, B., 1967. Si^{+4} content of natural phengite. Contrib. Mineral. Petrol. 14, 250–258.
Watson, E.B., Harrison, T.M., 1983. Zircon saturation revisited: temperature and composition effects in a variety of crustal magma types. Earth Planet. Sci. Lett. 64, 295–304.
Watson, E.B., Harrison, T.M., 2005. Zircon thermometer reveals minimum melting conditions on earliest Earth. Science 308, 841–844.
White, R.W., Powell, R.W., Holland, T.J.B., 2001. Calculation of partial melting equilibria in the system Na_2O–CaO–K_2O–FeO–MgO–Al_2O_3–SiO_2–H_2O (NCKFMASH). J. Metamorph. Geol. 19, 139–153.
Wilde, S.A., Valley, J.W., Peck, W.H., Graham, C.M., 2001. Evidence from detrital zircons for the existence of continental crust and oceans on the Earth 4.4 Gyr ago. Nature 409, 175–178.
Zahnle, K.J., 2006. Earth's earliest atmosphere. Elements 2, 217–222.